Renal nitric oxide production in rat pregnancy: role of constitutive nitric oxide synthases

Cheryl A. Smith,[1] Beth Santymire,[2] Aaron Erdely,[3] Vasuki Venkat,[4] György Losonczy,[5] and Chris Baylis[1,6]

[1]*Department of Physiology and Functional Genomics and* [6]*Department of Medicine, Division of Nephrology, University of Florida, Gainesville, Florida;* [2]*Department of Physiology, West Virginia University;* [3]*Toxicology and Molecular Biology Branch, National Institute of Occupational Safety and Health, Morgantown, West Virginia;* [4]*Department of Nephrology, University of California, San Diego, California; and* [5]*Department of Pulmonology, Semmelweis University, Budapest, Hungary*

Smith CA, Santymire B, Erdely A, Venkat V, Losonczy G, Baylis C. Renal nitric oxide production in rat pregnancy: role of constitutive nitric oxide synthases. *Am J Physiol Renal Physiol* 299: F830–F836, 2010. First published July 14, 2010; doi:10.1152/ajprenal.00300.2010.—Functional studies show that increased renal nitric oxide (NO) mediates the renal vasodilation and increased glomerular filtration rate that occur during normal pregnancy. We investigated whether changes in the constitutive NO synthases (NOS), endothelial (eNOS) and neuronal (nNOS), were associated with the increased renal NO production in normal midterm pregnancy in the rat. In kidneys from midterm pregnant (MP: 11–13 days gestation), late-term pregnant (LP: 18–20 days gestation), and similarly aged virgin (V) rats, transcript and protein abundance for eNOS and the nNOSα and nNOSβ splice variants, as well as the rate of L-arginine-to-L-citrulline conversion, were determined as a measure of NOS activity. At MP, renal cortical abundance of the total eNOS protein and phosphorylated (Ser^{1177}) eNOS was reduced, and L-arginine-to-L-citrulline conversion in the cortical membrane fraction was decreased; these declines were also seen in LP. There were no changes in the eNOS transcript. In contrast, L-arginine-to-L-citrulline conversion in the soluble fraction of renal cortex increased at MP and then declined at LP. This MP increase was ablated by *S*-methylthiocitrulline, a nNOS inhibitor. Using Western blotting, we did not detect a change in the protein abundance or transcript of the 160-kDa nNOSα, but protein abundance and transcript of the nNOSβ were increased at MP in cortex. Collectively, these studies suggest that the soluble nNOSβ is responsible for the increased renal cortical NO production during pregnancy.

endothelial nitric oxide synthase; neuronal nitric oxide synthase; L-arginine-to-L-citrulline conversion; *S*-methylthiocitrulline; splice variants

A MARKED RENAL VASODILATION occurs during pregnancy and leads to increases in renal plasma flow (RPF) and glomerular filtration rate (GFR) (5, 11, 13). In rats, this increase in RPF and GFR is maximal by midterm and involves a parallel relaxation of afferent and efferent arterioles (5, 11). Functional studies suggest that nitric oxide (NO) mediates the renal vasodilation, since nonselective NO synthase (NOS) inhibitors prevent the gestational rise in GFR (6, 9, 12, 14, 25).

Although NO appears to modulate the renal hemodynamic response during pregnancy, attempts to define the exact origin of the increased NO remain inconclusive. The use of isoform-"selective" NOS inhibitors has implicated neuronal and inducible NOS (nNOS and iNOS) (1, 3), while lack of endothelial NOS (eNOS)-selective inhibitors has prevented direct investigation of eNOS. Alexander et al. (4) reported an increase in nNOS protein abundance in rats at midterm, which coincides with maximal renal vasodilation (5), while an unexpected decline in eNOS protein abundance was also observed. In contrast, Novak et al. (27) reported no change in renal eNOS and nNOS protein abundance with pregnancy. Apart from the unresolved question of NOS protein abundance, large changes in NOS activity are possible without alterations in protein abundance. For example, phosphorylation of eNOS at Ser^{1177} can lead to a 15- to 20-fold increase in NOS activity compared with unphosphorylated eNOS (18).

To better our understanding of the renal NO system in pregnancy, we have conducted a series of studies assessing renal constitutive NOS isoform mRNA abundance, protein abundance, and activity in kidneys of virgin and pregnant rats.

MATERIALS AND METHODS

Animals. Studies were performed on female Sprague-Dawley rats (*n* = 51; Harlan Sprague Dawley, Indianapolis, IN) aged 4–5 mo. The animal studies were reviewed and approved by the West Virginia University and the University of Florida Animal Care and Use Committees. All animals were housed separately, provided rat chow and water ad libitum, and maintained on a 12:12-h light-dark cycle. Female rats were temporarily housed with males for 1–5 days. Mating was confirmed by the presence of sperm in the vagina (taken as *day 1* of pregnancy) and a continual diestrus vaginal smear. Pregnancy was confirmed by an increased body weight and the presence of live fetuses "in utero" on the day of death.

In *series 1*, in vitro NOS activity was evaluated in tissues harvested from midterm-pregnant (MP: 11–13 days gestation, *n* = 7), late-pregnant (LP: 18–20 days gestation, *n* = 8), and similarly aged virgin (V, *n* = 8) rats. In *series 2*, NOS mRNA and protein analysis was carried out in tissues harvested from MP (*n* = 5), LP (*n* = 5), and similarly aged V (*n* = 5) rats. In *series 3*, NOS mRNA and protein analysis was carried out in tissues harvested from MP (*n* = 4), LP (*n* = 4), and V (*n* = 5) rats.

Tissue harvest. Rats were anesthetized with pentobarbital sodium (0.7 mg/kg ip) or isoflurane. The kidneys were perfused blood-free with cold PBS, separated into cortex and medulla, flash frozen in liquid nitrogen, and stored at −80°C.

NOS activity. NOS activity was measured from the conversion of [^{3}H]L-arginine to [^{3}H]L-citrulline in kidney tissue, as described previously (32). Briefly, tissues were homogenized and ultracentrifuged. The supernatant (soluble) and membrane fractions were assayed. The soluble fraction contains most of the nNOS, while the membrane fraction contains mostly eNOS. Endogenous arginine was removed using Dowex, and the total protein content was determined using a Bradford assay (7). Samples were assayed in the presence of the

Address for reprint requests and other correspondence: C. Baylis, 1600 SW Archer Rd., Univ. of Florida, POB 100274, Gainesville, FL 32667 (e-mail: baylisc@ufl.edu).

arginase inhibitors valine (10 mM) and proline (10 mM). Data are expressed as picomoles of [^{3}H]L-arginine converted to [^{3}H]L-citrulline per milligram of protein per minute, adjusted for background. Background was determined by the amount of radioactivity obtained from heat-inactivated samples (60 min at 80°C) and represented <5% of the 100% standard, thus representing free tritium or noncationic tritiated species not bound by the Dowex resin. The 100% standards were prepared without Dowex and represented the total amount of counts available for conversion. Some samples were run in the presence of the nNOS-selective inhibitor *S*-methylthiocitrulline (SMTC, 1 μM).

Western blotting. Samples were homogenized, and proteins were separated by SDS-PAGE and transferred to a nitrocellulose membrane, as described previously (32). Ponceau S staining confirmed equivalent protein loads for cortex (200 μg of total protein) and medulla (100 μg of total protein). In *series 2*, membranes were first probed with rabbit polyclonal phosphorylated (Ser^{1177}) eNOS antibody (Cell Signaling Technology, Danvers, MA) in a 1:250 dilution of 5% BSA in 0.1% Tris-buffered saline + Tween 20 (TBS-T) for 16 h at 4°C and then with anti-rabbit IgG horseradish peroxidase (HRP)-linked antibody (Cell Signaling Technology) in a 1:2,000 dilution of 5% nonfat milk in 0.1% TBS-T for 1 h at room temperature. Membranes were then stripped and reprobed for eNOS (mouse monoclonal antibody, Transduction Laboratories, San Jose, CA) at a 1:250 dilution for 1 h. Next, goat anti-mouse IgG-HRP conjugate (Transduction Laboratories) at a 1:2,000 dilution was applied, and the membranes were incubated for 1 h. Duplicate membranes were run and probed for nNOS with a rabbit polyclonal antibody targeting the NH$_2$ terminus at a 1:5,000 dilution for 1 h (16) and then with goat anti-rabbit IgG-HRP (Bio-Rad, Hercules, CA) at a 1:3,000 dilution for 1 h at room temperature. In *series 3*, membranes were probed overnight with a 1:250 dilution of COOH-terminal rabbit polyclonal antibody (PA1–033, Affinity BioReagents, Golden, CO) or for 1 h with a 1:5,000 dilution of the same NH$_2$-terminal rabbit polyclonal antibody used in *series 2* (gift from Dr. Kim Lau) (22) and then for 1 h with a 1:3,000 dilution of secondary goat anti-rabbit IgG-HRP antibody (Bio-Rad). Bands of interest were visualized using an ECL Western blot detection kit (Amersham Biosciences, Piscataway, NJ). Densitometric analysis was performed using Optimas 6.2 imaging analysis software. Protein abundance is reported as integrated optical density (OD) units. The integrated OD was factored for Ponceau S staining (total protein loaded) and for an internal standard run on each membrane.

PCR. RNA was isolated from tissue using TRI Reagent (Sigma, St. Louis, MO) and treated with DNase I (Ambion, Austin, TX), and 1–2 μg was reversed transcribed (SuperScript II RNase H$^-$ Reverse Transcriptase, Invitrogen, Bethesda, MD) with random primers (Invitrogen) in a total volume of 20–40 μl. For control RT reactions, the RT enzyme was omitted, and primers were designed to include intron-exon splice sites. Primers were designed using GeneTool software (Biotools, Edmonton, AB, Canada) with annealing temperatures at 54–62°C. All PCR products were verified by restriction endonuclease digestion. Cyclophilin (CyP) was used as an internal reference, since CyP abundance remained consistent in V, MP, and LP rats.

For end-point PCR, preliminary experiments were conducted for each PCR product to ensure that the number of cycles represented the linear portion of the PCR OD curve. For each primer set [5′ acgccgctgtctctttc 3′ (forward) and 5′ tgccttctttcacccttc 3′ (reverse) for CyP (M19533), 5′ ccggctgccacctgatcctaacttg 3′ (forward) and 5′ tgcgcaatgtgagtccgaaaatgtc 3′ (reverse) for eNOS (XM342615), and 5′ cggccatcacgatattccctcag 3′ (forward) and 5′ cccgatctccagcagcatgttg 3′ (reverse) for "total" nNOS (NM052799); primer sets for nNOSα and nNOSβ were previously published (23, 30)], the cDNA from all samples was amplified simultaneously using aliquots from the same PCR mixture. PCR was carried out using 1 μg of cDNA, 50 ng of each primer, 250 μM deoxyribonucleotide triphosphates, 1× PCR buffer, and 2 U of *Taq* DNA polymerase (Sigma) in a 50-μl final volume. After amplification, 20 μl of each reaction were electropho-

resed on 1.5% agarose gels. Gels were stained with ethidium bromide, images were captured, and the signals were reported as arbitrary units (i.e., OD × band area) using the Kodak 1D image analysis system (Eastman Kodak, Rochester, NY). PCR signals were normalized to the CyP signal of the corresponding RT product to provide a semi-quantitative estimate of gene expression.

For two-step quantitative real-time PCR, Quantitect SYBR Green PCR reagents (Qiagen, Valencia, CA) were used according to the manufacturer's protocol on an iCycler iQ Multi-color Real-Time PCR Detection System (Bio-Rad). nNOS primers that would target all nNOS isoforms [5′ aagcctatgccaagaccctgtgtgagatc 3′ (forward) and 5′ ccagggcttcgtgctccaggtg 3′ (reverse) for total nNOS (NM052799), 5′ cggcgtgctgcgggatca 3′ (forward) and 5′ tgcggatgcggctcgtcac 3′ (reverse) for eNOS (XM342615), and 5′ gcccttgggtcgcgtctgct 3′ (forward) and 5′ caccctggcacatgaatcctgga 3′ (reverse) for CyP (M19533)] were designed. Real-time PCR, a more quantitative approach, was not used to detect nNOSα and nNOSβ mRNA, since multiple bands may occur with nNOSβ product amplification (30). Samples were run in duplicate (2.5–5 μl of cDNA per well), and the cycle times from duplicate wells were averaged. Preliminary experiments were conducted to optimize PCR conditions, ensure the absence of dimer formation, and affirm that a single PCR product was formed for each primer pair. For the relative quantification of gene expression, the comparative threshold cycle (C$_t$) method was employed (24). Validation methods were conducted over a 10-fold range of cDNA and over a 2-fold range of primer concentrations from control and experimental kidneys to confirm equal efficiency of NOS and CyP. The averaged NOS C$_t$ was subtracted from the corresponding averaged CyP C$_t$ for each sample, resulting in ΔC$_t$. The fold change was established by calculating $2^{-\Delta\Delta C_t}$ for experimental vs. control samples (16).

Statistical analysis. One-way ANOVA and Bonferroni's multiple comparison test were used to compare mRNA and protein abundance differences of V, MP, and LP samples. Values are means ± SE. Significance was accepted at $P < 0.05$.

RESULTS

As shown in Fig. 1, the abundance of total eNOS (Fig. 1*A*) and phosphorylated eNOS (Fig. 1*B*) falls during pregnancy in renal cortex. In renal medulla, there were no significant changes in eNOS or phosphorylated eNOS abundance (Fig. 1, *C* and *D*). Representative blots for renal medulla in Fig. 1, *E* and *F*, show that the eNOS antibody recognized the eNOS- and phosphorylated eNOS-positive controls (*lanes 1* and *2* in Fig. 1*E*), while the phosphorylated (Ser^{1177}) eNOS antibody recognized only the phosphorylated eNOS-positive control (*lane 1* in Fig. 1*F*). To measure eNOS transcript, we used CyP mRNA abundance as an internal control for end-point and real-time PCR, since CyP mRNA abundance did not change with pregnancy (Table 1). Cortical and medullary eNOS mRNA abundance was unaffected by pregnancy, as shown by end-point and real-time PCR and two different primer pairs (Table 1).

We measured the total [^{3}H]L-arginine-to-[^{3}H]L-citrulline conversion, as a measure of NOS activity, in renal cortex and medulla membrane fractions (Fig. 2). [^{3}H]L-arginine-to-[^{3}H]L-citrulline conversion was significantly lower in LP than V rats in cortex. In medulla, membrane NOS activity fell in pregnancy. There was, however, a significant increase in [^{3}H]L-arginine-to-[^{3}H]L-citrulline conversion in the soluble fraction of renal cortex of MP compared with V and LP rats (Fig. 3). In MP rats, the nNOS-selective NOS inhibitor SMTC reduced the cortical soluble [^{3}H]L-arginine-to-[^{3}H]L-citrulline conversion to V values. In medulla, there was no difference in total NOS activity in the soluble fraction during pregnancy, and SMTC
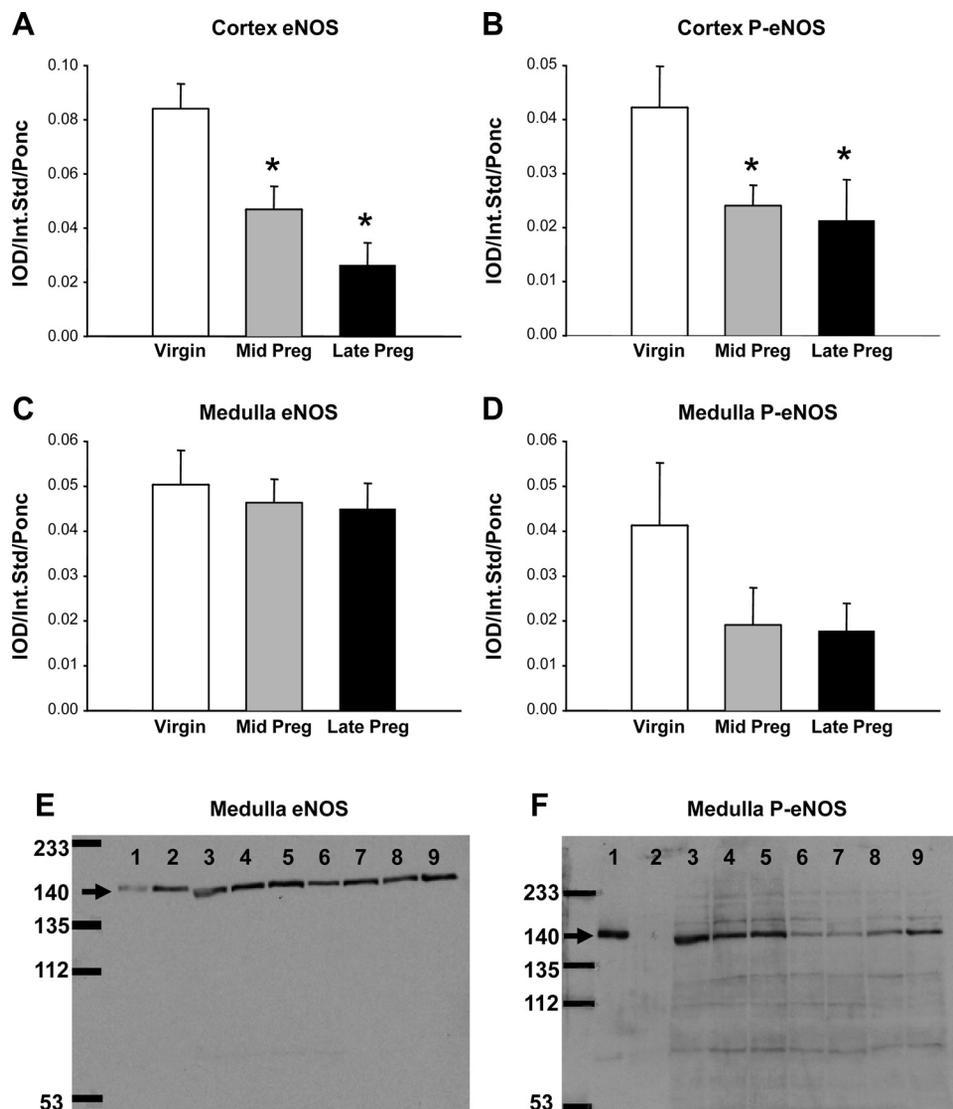
Fig. 1. Relative abundance of kidney endothelial nitric oxide synthase (eNOS) and phosphorylated (Ser[1177]) eNOS (P-eNOS) in cortex and medulla of virgin, midterm pregnant (Mid Preg), and late-term pregnant (Late Preg) rats. *A–D*: average densitometric values [integrated optical density (IOD)/internal standard (Int Std)/Ponceau S (Ponc)] for eNOS and P-eNOS in renal cortex and medulla. *Significantly different from virgin ($P < 0.05$). *E* and *F*: representative Western blots for eNOS and P-eNOS in renal medulla. A molecular weight marker (in kDa) is shown at *far left*. *Lane 1*, P-eNOS-positive control (lysate of VEGF-treated rat aortic endothelial cells); *lane 2*, eNOS-positive control (lysate of confluent unstimulated rat aortic endothelial cells); *lanes 3* and *4*, virgin; *lanes 5* and *6*, midterm pregnant; *lanes 7–9*, late-term pregnant.

inhibited >50% of [³H]L-arginine-to-[³H]L-citrulline conversion in V, MP, and LP rats.

We also measured cortical and medullary nNOSα protein abundance. As shown in Fig. 4, *A* and *B*, there was no change in nNOSα protein abundance with pregnancy in animals in *series 3* or in animals in *series 2* (data not shown). In contrast, there was a marked rise in the cortical nNOSβ protein abundance at MP (Fig. 4*C*) that occurred in parallel with the increase in NOS activity in the soluble fraction of cortex (Fig. 3). Representative blots for the nNOSα and nNOSβ proteins

Table 1. *mRNA abundance: series 2 experiments*

	Renal Cortex			Renal Medulla		
	V	MP	LP	V	MP	LP
Real-time PCR						
eNOS*		0.88	0.85		0.86	0.68
nNOS*		1.04	1.10		0.84	0.78
CyP†	19.28 ± 0.15	19.38 ± 0.38	17.59 ± 0.45	17.92 ± 0.06	17.68 ± 0.06	17.72 ± 0.06
End-point PCR‡						
eNOS	0.37 ± 0.04	0.43 ± 0.07	0.36 ± 0.04	0.87 ± 0.19	0.87 ± 0.15	0.73 ± 0.04
nNOS	0.71 ± 0.15	0.71 ± 0.14	0.69 ± 0.14	0.78 ± 0.06	0.76 ± 0.02	0.70 ± 0.04
CyP	2.72 ± 0.38	2.80 ± 0.58	2.54 ± 0.47	2.19 ± 0.18	2.37 ± 0.13	2.33 ± 0.10

V, virgin; MP, midterm pregnant; LP, late-term pregnant; eNOS and nNOS, endothelial and neuronal nitric oxide synthase; CyP, cyclophilin. *eNOS and nNOS real-time PCR values are expressed as mean fold change in gene expression ($2^{-\Delta\Delta Ct}$, where C_t is cycle time) compared with V. †CyP real-time PCR values (means ± SE) are expressed in C_t. ‡End-point PCR values (means ± SE) are expressed in arbitrary units; eNOS and nNOS were normalized to CyP.
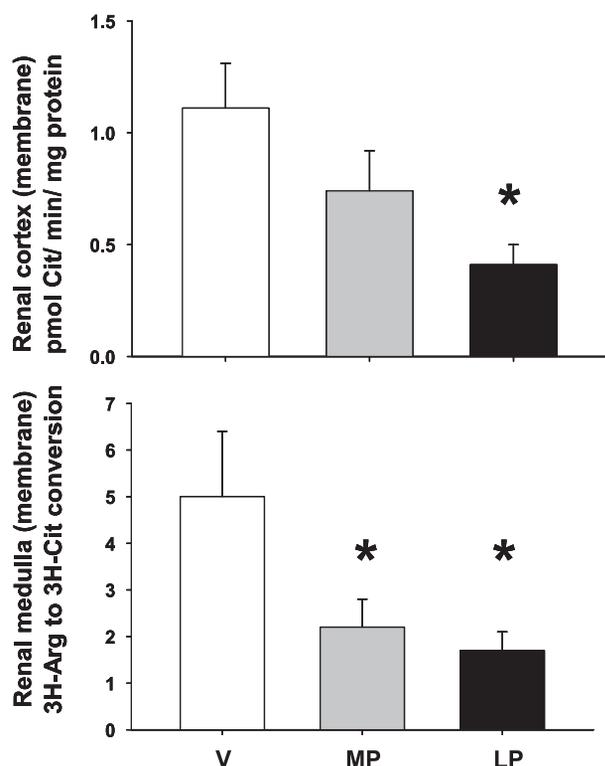
Fig. 2. Rate of conversion of [^{3}H]L-arginine to [^{3}H]L-citrulline as a measure of NOS activity in membrane fraction of renal cortex and medulla of virgin (V), midterm pregnant (MP), and late-term pregnant (LP) rats. *Significantly different from V ($P < 0.05$).

(from animals in *series 3*) are shown in Fig. 5. The total nNOS transcript was unchanged by real-time and end-point PCR (Table 1), and there was no change in nNOSα mRNA in cortex or medulla during pregnancy, while nNOSβ transcript increased in cortex and medulla in MP rats (Fig. 6).

DISCUSSION

The main findings in the present study are that, in renal cortex of the MP rat, membrane NOS activity and total and phosphorylated (Ser^{1177}) eNOS protein are not increased when the gestational renal vasodilation is at a maximum. In contrast, a marked rise in renal cortical NOS activity in the soluble fraction is evident, which can be ablated with SMTC, a nNOS-selective inhibitor (17, 26). Using an antibody to the NH$_2$ terminus of the 160-kDa nNOSα, we saw no change in protein expression during pregnancy, and the nNOSα transcript was also unchanged. Transcript and protein abundance of the functional splice variant nNOSβ was significantly elevated in renal cortex at MP, coincident with the gestational renal vasodilation.

Our findings confirm earlier observations that increased eNOS expression does not contribute to the NO-dependent renal vasodilation and hyperfiltration that occurs during pregnancy. Previous studies indicate no change (27) or a decrease (4) in eNOS during pregnancy. Here, we report decreases in total cortical eNOS abundance at MP and LP, and we found no change in eNOS transcript abundance. Of course, protein abundance is not the only determinant of eNOS activity, since there are many possible posttranslational modifications that affect activity, including phosphorylation of eNOS at Ser^{1177},

which increases activity by 15- to 20-fold (18). However, we found that the abundance of phosphorylated eNOS also falls in renal cortex during pregnancy. Since two different antibodies detected falls in eNOS and phosphorylated eNOS abundance in pregnancy, we conclude that decreased eNOS protein probably accounts for the decrease in renal cortical membrane NOS activity also seen in this study. Thus, surprisingly, the NO-dependent renal vasodilation of pregnancy in the rat is not due to the eNOS.

In contrast to the membrane fraction, we observed a significant increase in renal cortical soluble NOS activity at MP and a return in LP that parallels the time course of the gestational renal vasodilation in the rat (5, 11). iNOS and some nNOS reside in the soluble fraction. We used a relatively selective nNOS inhibitor (SMTC, K_i = 1.2 nM), which have been reported to exhibit >100-fold selectivity for rat nNOS compared with iNOS, ~10-fold selectivity for nNOS over eNOS in purified enzyme preparations, and 17-fold selectivity for nNOS over eNOS in tissues (17, 26). We found that SMTC completely prevented the rise in soluble NOS activity in renal cortex in MP while having no impact on V or LP tissue homogenates. This suggests that the increased soluble NOS activity originated from a nNOS source. These findings are in agreement with studies by Abram and colleagues (1), who reported that acute infusion of another nNOS-selective inhibitor, 7-nitroindazole, decreased RPF and GFR in conscious pregnant rats without affecting renal hemodynamics of virgins. Although SMTC and 7-nitroindazole are chemically unrelated, both are used as selective nNOS inhibitors (17). As a cautionary note, however, assumptions based on supposedly "isoform-selective" NOS inhibitors are fraught with problems. Alderton
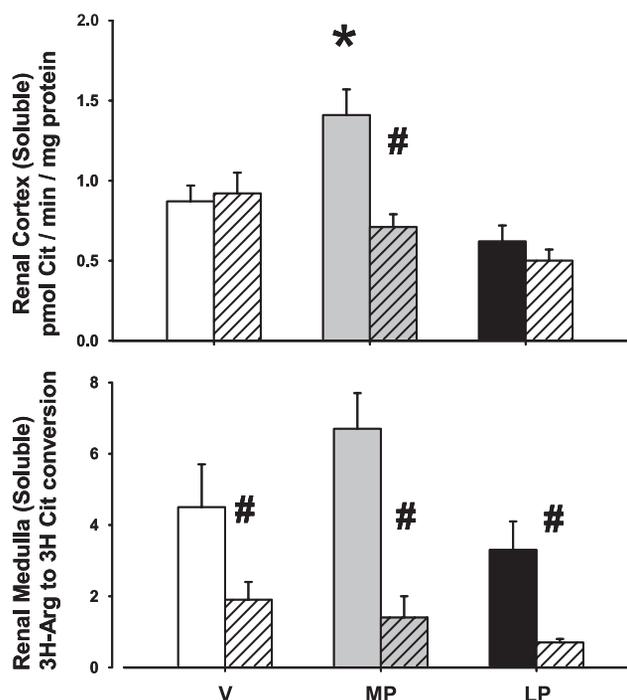

Fig. 3. Rate of conversion of [^{3}H]L-arginine to [^{3}H]L-citrulline as a measure of NOS activity in soluble fraction of renal cortex and medulla. Solid columns, baseline state; hatched columns, *S*-methylthiocitrulline. *Significantly different from V and LP ($P < 0.05$). #Significantly different from baseline ($P < 0.05$).

Fig. 4. *A* and *B*: relative neuronal NOS (nNOS)-α (nNOSα) protein abundance in *series 3* rats (i.e., NH$_2$-terminal antibody) in cortex and medulla in V, MP, and LP rats. *C* and *D*: relative nNOSβ abundance in cortex and medulla. nNOS-positive control is rat cerebellar lysate. ◆Significantly different from V ($P < 0.05$).
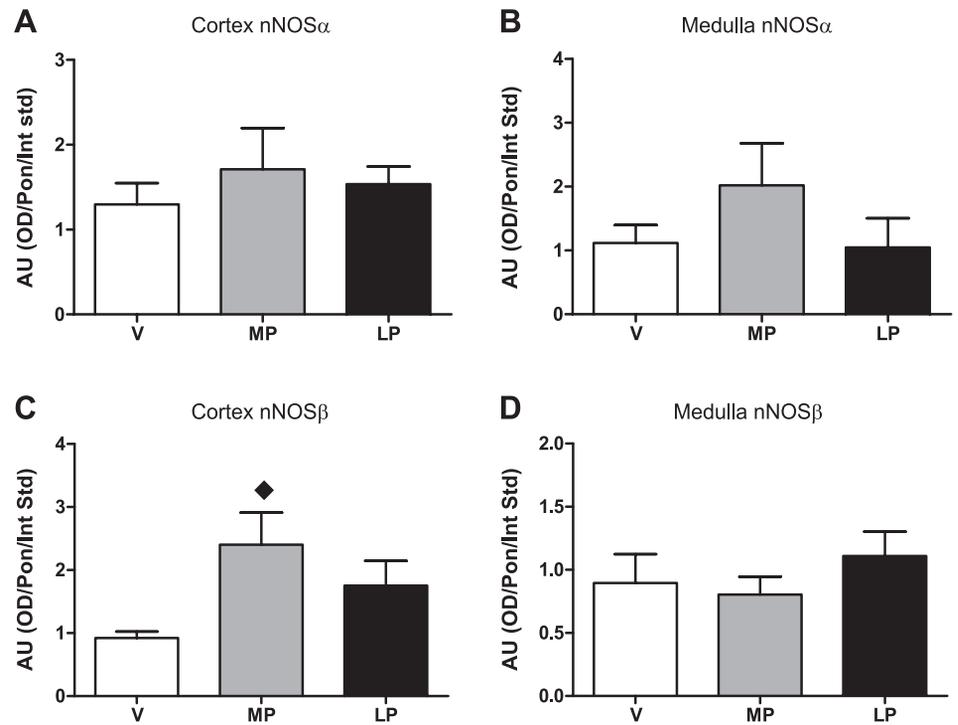
et al. (2) report that much of the confusion results from the differing criteria used to define selectivity. In fact, when selectivity is defined on the basis of potency under identical conditions and in the physiological range, few selective NOS inhibitors are highly selective. This may explain why nNOS-selective (1) and iNOS-selective (3) inhibitors have been shown to ablate the gestational rise in GFR. In view of this, we cannot rely on selective NOS inhibitors as a means of defining which NOS isoform(s) play(s) a role in renal hemodynamic changes that occur with pregnancy; therefore, we also looked at NOS protein and transcript abundance.

Novak et al. (27) reported no change in medullary nNOS protein abundance and could not detect the nNOS protein in renal cortex in V or MP; they observed no change in the cortical nNOS transcript in MP vs. V. In contrast, Alexander et

al. (4) reported a significant increase in whole kidney nNOS protein abundance that reached a peak at midterm (13 days gestation) and remained high throughout the rest of pregnancy. These workers used a commercially available antibody to the COOH terminus of nNOS, which we now recognize will detect all the nNOS splice variants that are present. In the present study, using an antibody to nNOSα (which recognizes only the unique NH$_2$ terminus of nNOSα), we found no change in protein abundance at MP, and this was confirmed at the transcript level.

We recently reported that there are nNOS splice variants in the normal rat kidney and that the proportions of these can change under pathological conditions (30). Of particular relevance to the present study, one of these splice variants, nNOSβ, is a functional enzyme that is entirely cytosolic in

Fig. 5. *Top*: representative whole membrane Western blots of renal cortex (300 µg of total protein) and medulla (100 µg of total protein). An NH$_2$-terminal antibody (22) was used for nNOSα (~160 kDa, arrowhead) detection (*A*), and a COOH-terminal antibody (PA1–033, Affinity Bioreagents) was used for nNOSβ (~140 kDa, arrow) detection (*B*). *Bottom*: Ponceau S staining of corresponding lanes confirming similar protein loads.
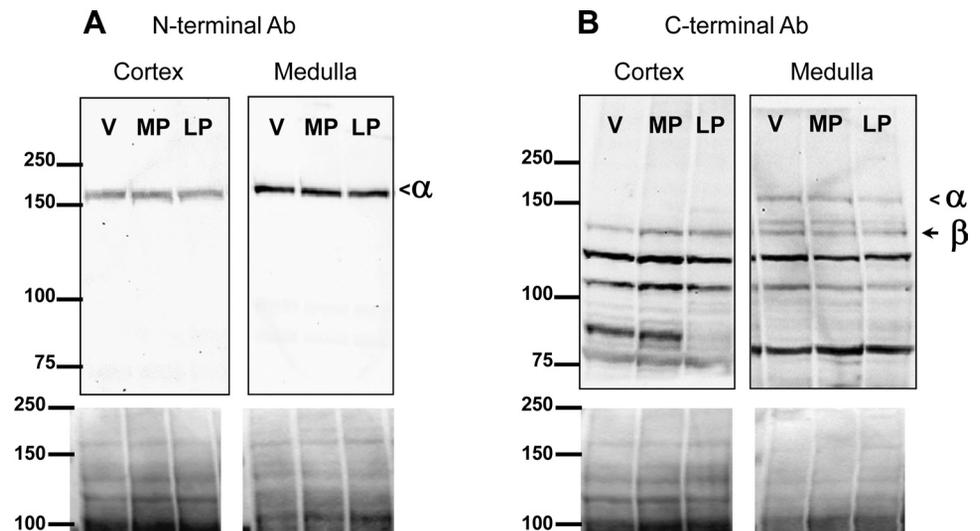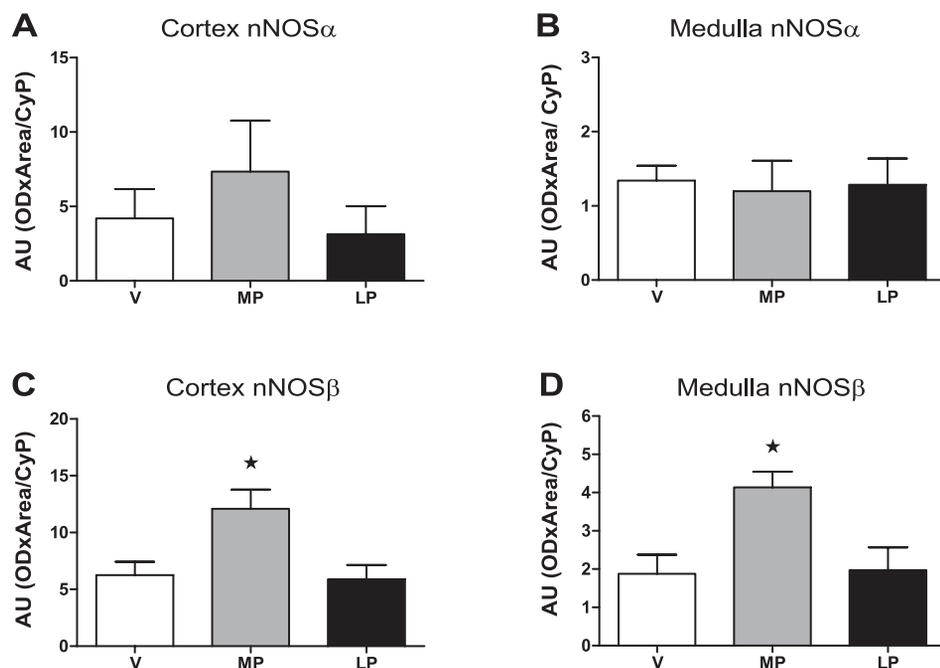
Fig. 6. Relative nNOSα and nNOSβ mRNA abundance in renal cortex (*A* and *C*) and medulla (*B* and *D*) assessed by end-point PCR. There was no significant difference in cortical or medullary nNOSα mRNA abundance between V, MP, and LP. However, nNOSβ mRNA abundance was significantly increased in MP rats compared with V and LP rats. AU, arbitrary units [i.e., optical density (OD) × area/cyclophilin (CyP)]. *Significantly different from V and LP ($P < 0.05$).

location (2). Lacking the unique PDZ-binding domain at the NH_2 terminus, nNOSβ would be recognized by antibodies targeting the COOH, but not the NH_2, terminus. We therefore conducted a preliminary study assessing the variable 5′-untranslated regions (5′-UTRs; exon 1a, 1b, and 1c) reported by Lee and colleagues (23) in the rat kidney. Using RT-PCR and exon 1a-exon 6 primer pairing, we detected two bands, indicating that nNOSα and nNOSβ transcripts had a common 5′-UTR (30), as previously reported by Huber et al. (19) in the rat small intestine. Although we report no change in nNOSα transcript abundance with exon 1a-exon 2 primer pairing and a significant increase in nNOSβ transcript abundance at MP with exon 1a-exon 6 primer pairing, we recognize that there may be additional transcripts for nNOSα and nNOSβ. Indeed, in rat kidney, Lee et al. (23) identified three nNOS transcripts with distinct 5′-UTR first exons (exon 1a, 1b, and 1c), all of which spliced to exon 2 (nNOSα). Oberbaumer et al. (28) identified five nNOS mRNA variants: four encoded for nNOSα (exon 2), and one encoded for nNOSβ (exon 3). Although these nNOS mRNA variants may be generated by alternative promoters encoding the same nNOS protein, it is possible that the various nNOS transcripts with different 5′-UTRs may have different functional properties that may influence mRNA translational efficiency, alter mRNA localization, or alter mRNA stability. This may account for the differences in cortical and medullary nNOSα and nNOSβ transcript expression compared with nNOSα and nNOSβ protein abundance seen in the present study.

We used the previously characterized COOH-terminal nNOS antibody (30) to directly test whether nNOSβ might contribute to the gestational renal vasodilation and observed a marked increase in the protein abundance. Unlike the nNOSα, nNOSβ contains a unique NH_2 terminus of 6 amino acids and lacks the first 236 amino acids of nNOSα, which contains the PSD-95 disks large/ZO-1 homology (PDZ) and protein inhibitor of NOS (PIN) domains. The PDZ domain of nNOSα mediates interaction with postsynaptic density protein 95

(PSD-95) of neurons and $α_1$-syntrophin (part of the dystrophin complex) of myocytes, which anchors nNOSα in the plasma membrane (8). Without a PDZ domain, nNOSβ would occur in the cytosol, as shown by Huber et al. (19) in the rat intestine. Furthermore, the PIN domain contains a binding site for the protein inhibitor of NOS (21), and without a PIN domain, nNOSβ cannot be regulated by PIN. Therefore, nNOSβ may be regulated by other mechanisms, such as alternate promoter usage and pre-mRNA splicing events (31). With no PDZ and PIN domains, the secondary and/or tertiary structure of nNOSβ may be similar to iNOS, and we speculate that iNOS-selective inhibitors may inhibit the activity of iNOS and nNOSβ. Also, with similar molecular weights, nNOSβ may comigrate with iNOS and/or be mistaken for iNOS in the absence of appropriate positive controls.

Brenman and colleagues (8) reported that nNOSβ transfected in COS cells was catalytically active, with a K_m for arginine similar to nNOSα, and fully dependent on calcium/calmodulin. Several in vivo studies using wild-type and nNOSα$^{-/-}$ mice also suggested a functional role for nNOSβ. For example, in wild-type mice, nNOSβ is a functional enzyme accounting for much of the citrulline formation in many brain areas (15). The nNOSα$^{-/-}$ and eNOS$^{-/-}$ double-knockout mice exhibit normal penile erection mediated by nNOSβ (20). In nNOSα$^{-/-}$ mice, nNOSβ abundance increases, suggesting a compensatory upregulation of nNOSβ when nNOSα-derived NO is deficient (15). In humans, nNOSβ has been localized in the spinal cord and is upregulated in astrocytes of the ventral horn and white matter in patients with amyotrophic lateral sclerosis (10). This suggests that nNOSβ may be upregulated in disease states, as also reported by us in the rat kidney with chronic kidney disease (30). The present study suggests that renal cortex nNOSβ is upregulated in response to physiological stimuli in normal pregnancy, which we suggest may play an important role in the renal vasodilation at MP.

In summary, the increase in renal cortical NO generation during pregnancy cannot be attributed to increased abundance

or activity of eNOS. Rather, nNOSβ in the soluble fraction of renal cortex provides the likely source. Future studies should investigate the specific location and the signaling pathway responsible for activating the renal cortical nNOSβ in normal pregnancy.

DISCLOSURES

No conflicts of interest, financial or otherwise, are declared by the authors.

REFERENCES

1. **Abram SR, Alexander BT, Bennett WA, Granger JP.** Role of neuronal nitric oxide synthase in mediating renal hemodynamic changes during pregnancy. *Am J Physiol Regul Integr Comp Physiol* 281: R1390–R1393, 2001.
2. **Alderton WK, Cooper CE, Knowles RG.** Nitric oxide synthases: structure, function and inhibition. *Biochem J* 357: 593–615, 2001.
3. **Alexander BT, Cockrell K, Cline FD, Granger JP.** Inducible nitric oxide synthase inhibition attenuates renal hemodynamics during pregnancy. *Hypertension* 39: 586–590, 2002.
4. **Alexander BT, Miller MT, Kassab S, Novak J, Reckelhoff JF, Kruckeberg WC, Granger JP.** Differential expression of renal nitric oxide synthase isoforms during pregnancy in rats. *Hypertension* 33: 435–439, 1999.
5. **Baylis C.** Glomerular filtration and volume regulation in gravid animal models. *Baillieres Clin Obstet Gynaecol* 8: 235–264, 1994.
6. **Baylis C, Engels K.** Adverse interactions between pregnancy and a new model of systemic hypertension produced by chronic blockade of endothelial derived relaxing factor (EDRF) in the rat. *Clin Exp Hypertens* B11: 117–129, 1992.
7. **Bradford MM.** A rapid and sensitive method for the quantitation of microgram quantities of protein utilizing the principle of protein-dye binding. *Anal Biochem* 72: 248–254, 1976.
8. **Brenman JE, Chao DS, Gee SH, McGee AW, Craven SE, Santillano DR, Wu Z, Huang F, Xia H, Peters MF, Froehner SC, Bredt DS.** Interaction of nitric oxide synthase with the postsynaptic density protein PSD-95 and α₁-syntrophin mediated by PDZ domains. *Cell* 84: 757–767, 1996.
9. **Cadnapaphornchai MA, Ohara M, Morris KG Jr, Knotek M, Rogachev B, Ladtkow T, Carter EP, Schrier RW.** Chronic NOS inhibition reverses systemic vasodilation and glomerular hyperfiltration in pregnancy. *Am J Physiol Renal Physiol* 280: F592–F598, 2001.
10. **Catania MV, Aronica E, Yankaya B, Troost D.** Increased expression of neuronal nitric oxide synthase spliced variants in reactive astrocytes of amyotrophic lateral sclerosis human spinal cord. *J Neurosci* 21: RC148, 2001.
11. **Conrad KP.** Renal hemodynamics during pregnancy in chronically catheterized, conscious rats. *Kidney Int* 26: 24–29, 1984.
12. **Danielson LA, Conrad KP.** Acute blockade of nitric oxide synthase inhibits renal vasodilation and hyperfiltration during pregnancy in chronically instrumented conscious rats. *J Clin Invest* 96: 482–490, 1995.
13. **Davison JM, Dunlop W.** Renal hemodynamics and tubular function normal human pregnancy. *Kidney Int* 18: 152–161, 1980.
14. **Deng A, Engels K, Baylis C.** Impact of nitric oxide deficiency on blood pressure and glomerular hemodynamic adaptations to pregnancy in the rat. *Kidney Int* 50: 1132–1138, 1996.
15. **Eliasson MJ, Blackshaw S, Schell MJ, Snyder SH.** Neuronal nitric oxide synthase alternatively spliced forms: prominent functional localizations in the brain. *Proc Natl Acad Sci USA* 94: 3396–3401, 1997.
16. **Erdely A, Freshour G, Smith C, Engels K, Olson JL, Baylis C.** Protection against puromycin aminonucleoside-induced chronic renal disease in the Wistar-Furth rat. *Am J Physiol Renal Physiol* 287: F81–F89, 2004.
17. **Furfine ES, Harmon MF, Paith JE, Knowles RG, Salter M, Kiff RJ, Duffy C, Hazelwood R, Oplinger JA, Garvey EP.** Potent and selective inhibition of human nitric oxide synthases. Selective inhibition of neuronal nitric oxide synthase by S-methyl-L-thiocitrulline and S-ethyl-L-thiocitrulline. *J Biol Chem* 269: 26677–26683, 1994.
18. **Gallis B, Corthals GL, Goodlett DR, Ueba H, Kim F, Presnell SR, Figeys D, Harrison DG, Berk BC, Aebersold R, Corson MA.** Identification of flow-dependent endothelial nitric-oxide synthase phosphorylation sites by mass spectrometry and regulation of phosphorylation and nitric oxide production by the phosphatidylinositol 3-kinase inhibitor LY294002. *J Biol Chem* 274: 30101–30108, 1999.
19. **Huber A, Saur D, Kurjak M, Schusdziarra V, Allescher HD.** Characterization and splice variants of neuronal nitric oxide synthase in rat small intestine. *Am J Physiol Gastrointest Liver Physiol* 275: G1146–G1156, 1998.
20. **Hurt KJ, Sezen SF, Champion HC, Crone JK, Palese MA, Huang PL, Sawa A, Luo X, Musicki B, Snyder SH, Burnett AL.** Alternatively spliced neuronal nitric oxide synthase mediates penile erection. *Proc Natl Acad Sci USA* 103: 3440–3443, 2006.
21. **Jaffrey SR, Snyder SH.** PIN: an associated protein inhibitor of neuronal nitric oxide synthase. *Science* 274: 774–777, 1996.
22. **Lau KS, Grange RW, Isotani E, Sarelius IH, Kamm KE, Huang PL, Stull JT.** nNOS and eNOS modulate cGMP formation and vascular response in contracting fast-twitch skeletal muscle. *Physiol Genomics* 2: 21–27, 2000.
23. **Lee MA, Cai L, Hubner N, Lee YA, Lindpaintner K.** Tissue- and development-specific expression of multiple alternatively spliced transcripts of rat neuronal nitric oxide synthase. *J Clin Invest* 100: 1507–1512, 1997.
24. **Livak KJ, Schmittgen TD.** Analysis of relative gene expression data using real-time quantitative PCR and the $2^{-\Delta\Delta C_T}$ method. *Methods* 25: 402–408, 2001.
25. **Molnar M, Hertelendy F.** Nω-nitro-L-arginine, an inhibitor of nitric oxide synthesis, increases blood pressure in rats and reverses the pregnancy-induced refractoriness to vasopressor agents. *Am J Obstet Gynecol* 166: 1560–1567, 1992.
26. **Narayanan K, Griffith OW.** Synthesis of L-thiocitrulline, L-homothiocitrulline, and S-methyl-L-thiocitrulline: a new class of potent nitric oxide synthase inhibitors. *J Med Chem* 37: 885–887, 1994.
27. **Novak J, Rajakumar A, Miles TM, Conrad KP.** Nitric oxide synthase isoforms in the rat kidney during pregnancy. *J Soc Gynecol Investig* 11: 280–288, 2004.
28. **Oberbaumer I, Moser D, Bachmann S.** Nitric oxide synthase 1 mRNA: tissue-specific variants from rat with alternative first exons. *Biol Chem* 379: 913–919, 1998.
29. **Singh R, Pervin S, Rogers NE, Ignarro LJ, Chaudhuri G.** Evidence for the presence of an unusual nitric oxide- and citrulline-producing enzyme in rat kidney. *Biochem Biophys Res Commun* 232: 672–677, 1997.
30. **Smith C, Merchant M, Fekete A, Nyugen HL, Oh P, Tain YL, Klein JB, Baylis C.** Splice variants of neuronal nitric oxide synthase are present in the rat kidney. *Nephrol Dial Transplant* 24: 1422–1428, 2009.
31. **Wang Y, Newton DC, Robb GB, Kau CL, Miller TL, Cheung AH, Hall AV, VanDamme S, Wilcox JN, Marsden PA.** RNA diversity has profound effects on the translation of neuronal nitric oxide synthase. *Proc Natl Acad Sci USA* 96: 12150–12155, 1999.
32. **Xiao S, Erdely A, Wagner L, Baylis C.** Uremic levels of BUN do not cause nitric oxide deficiency in rats with normal renal function. *Am J Physiol Renal Physiol* 280: F996–F1000, 2001.